

LINEARIZED AEROSERVOELASTIC ANALYSIS OF ROTARY-WING AIRCRAFT

Pierangelo Masarati, Vincenzo Muscarello, Giuseppe Quaranta

Dipartimento di Ingegneria Aerospaziale, Politecnico di Milano
 {masarati,muscarello,quaranta}@aero.polimi.it

Abstract

A tool for the aeroservoelastic analysis of rotary-wing aircraft, including tiltrotors, is presented. Rather than developing yet an entirely new, monolithic rotorcraft aeroservoelastic simulation software, capable of providing all the modeling capabilities required by modern rotorcraft, each separate feature has been collected from well-known, reliable and possibly state-of-art sources and blended together in a general-purpose mathematical environment. The resulting intrinsic modularity allows to easily incorporate improved features as required by specific problems. In particular the tool can be very effective for aeroservoelastic stability analysis, development and tuning of dynamic controllers and investigation of aeroelastic coupling with Flight Control Systems. The implementation of state-space aircraft aeroservoelastic numerical models into a general purpose mathematical environment allows to exploit state-space based modern control theory approaches.

INTRODUCTION

Despite the possibility of improving the mission effectiveness of rotorcraft, the development of full-authority Flight Control Systems (FCS) is lagging behind the evolution of the similar systems for fixed wing aircraft. However, the expected enhancements in terms of handling qualities and reduction of pilot workload, with the promise of increased safety, are increasing the number of production fly-by-wire rotorcraft [1]. The introduction of FCS requires to include it in the aircraft design phase to verify that it does not compromise the overall aeroelastic stability and vibratory level of the aircraft. Insertion of appropriate notch filters needs to be thoroughly investigated to prevent any spillover effect caused by the FCS gain at aeroelastic mode frequencies [2]. To perform this kind of analysis, reliable but fast numerical approaches need to be considered. They must allow to investigate the interaction among different subsystems like deformable mechanical components, servo-hydraulic elements, unsteady aerodynamic forces, pilot models, control logic and so on.

Several numerical approach with different levels of sophistication have been implemented in the past to study rotorcraft aeromechanics. Noteworthy examples are presented in [3, 4, 5, 6, 7]. Perhaps a less general, more "control oriented" approach is represented by ASAP [8], developed to investigate structural coupling problems for tiltrotor

fly-by-wire architectures.

In this work, instead of developing yet an entirely new rotorcraft aeroservoelastic simulation software, a simulation tool has been built on top of the general-purpose mathematical environment MATLAB. The tool can perform massive analyses of relatively simple, yet complete modular models of complex linearized aeroservoelastic systems. Each separate model component consists of submodels collected from well-known, reliable and possibly state-of-art sources, and blended together, rather than deriving them from first principles equations. All blocks are represented as differential equations in state-space form. The intrinsic modularity allows several advantages:

- a broad range of approximation levels for each sub-system; different sources of increasing sophistication can be used to assemble models for the same component; this allows line up with the state-of-the-art;
- ease in model expansion to include additional components;
- access to the huge library of controls analysis and synthesis and optimization tool available in MATLAB.

The resulting multidisciplinary models can be used for the design of control systems for flutter suppression, vibration reductions and load alleviation.

The result of this work is MASST (Modern Aeroservoelastic State-Space Tools), a collection of tools developed by Politecnico di Milano for the linearized aeroservoelastic analysis of fixed and rotary-wing aircraft, based on the state-space approach, often indicated as “modern” in the automatic control community. In fact, since a time domain formulation in the state-space is the core of the modern control theory, the equations of motion of the system are cast as first order time differential equations. Once this is accomplished, it is no longer necessary to use the specialized formulations generally adopted in aeroelastic analysis; general state-space approaches can be rather used to analyze aeroelastic systems.

MULTIDISCIPLINARY MODEL

MASST has been designed to be modular and to allow to incorporate heterogeneous sub-components from different sources to model:

1. airframe structural dynamics, including unsteady aerodynamics;
2. rotors aeroelasticity;
3. drive train;
4. servo-actuators;
5. sensors and filters;
6. Flight Control Systems (FCS);
7. pilot biomechanics.

For each element type, an arbitrary number of blocks can be added to the main model, to allow to build aircraft models of arbitrary architecture. Figure 1 shows a block scheme of the sub-components used to model a tiltrotor. Items 1–3 provide the core of basic aeroelastic analysis capabilities. Items 1–4 provide aeroservoelastic analysis capabilities. Items 1–7 provide closed loop aeroservoelastic capabilities.

Each component is modeled in its most natural and appropriate modeling environment and then cast into first order state-space formulation. Substructures are then connected using the Craig-Bampton Component Mode Synthesis (CMS) approach [9].

Airframe Structural Dynamics

The non-rotating aeroelastic subsystems can be logically split in structural and aerodynamic models, since the structural model does not depend on

the flight condition, while the aerodynamic model can be parametrized on flow parameters, e.g. Mach number and dynamic pressure. The airframe structural models are represented by a Reduced Order Model (ROM) obtained using the classical Ritz decomposition for the displacement field \mathbf{u}

$$\mathbf{u}(\mathbf{x}, t) = \mathbf{U}(\mathbf{x})\mathbf{q}(t), \quad (1)$$

based on a compact set of selected generalized coordinates \mathbf{q} . Usually the model is obtained by reducing a detailed Finite Element Model (FEM) using displacement shapes \mathbf{U} chosen among the normal vibration modes of the structure, complemented with additional *constraint modes*, namely static shapes specifically designed to represent local effects, or control modes that represent the motion of control surfaces. The structural dynamics is thus represented by

$$\mathbf{M}_{\mathbf{q}\mathbf{q}}\ddot{\mathbf{q}} + \mathbf{C}_{\mathbf{q}\mathbf{q}}\dot{\mathbf{q}} + \mathbf{K}_{\mathbf{q}\mathbf{q}}\mathbf{q} = \mathbf{f}, \quad (2)$$

where matrices $(\cdot)_{\mathbf{q}\mathbf{q}}$ are symmetric, but in general fully populated since no orthogonality is required to the forms \mathbf{U} . The airframe structure can be composed by an arbitrary number of substructures connected using the CMS. The aim is twofold: a) to parametrize the model in terms of the relative orientation of parts, as required by tiltrotor nacelles; b) to be able to temporarily add and remove sub-components like pylons or appendages.

Unsteady Aerodynamics. Unsteady aerodynamic forces associated to small motion of the airframe and gusts can be obtained as solutions of integro-differential equations related to harmonic boundary domain oscillation, namely the generalized aerodynamic forces frequency responses \mathbf{f}_a .

$$\mathbf{f}_a = q_\infty \mathbf{H}_{am}(k, M_\infty)\mathbf{q} + q_\infty \mathbf{H}_{ag}(k, M_\infty)\mathbf{v}_g, \quad (3)$$

where q_∞ is the dynamic pressure, $k = \omega c / (2V_\infty)$ is the reduced frequency, M_∞ is the Mach number, \mathbf{H}_{am} and \mathbf{H}_{ag} are the aerodynamic transfer matrices associated to the structural mode shapes \mathbf{q} and to the gust input \mathbf{v}_g . Matrices \mathbf{H}_{am} and \mathbf{H}_{ag} can be obtained using the classical Doublet Lattice Method (DLM) of NASTRAN, but also CFD as shown for example in [10].

MASST can cast the resulting frequency domain matrices in state-space form

$$\dot{\mathbf{x}}_a = \mathbf{A}_a \mathbf{x}_a + \mathbf{B}_a \mathbf{a} \quad (4a)$$

$$\frac{\mathbf{f}_a}{q_\infty} = \mathbf{C}_a \mathbf{x}_a + \mathbf{D}_{a0} \mathbf{a} + \frac{c}{2V_\infty} \mathbf{D}_{a1} \dot{\mathbf{a}} + \left(\frac{c}{2V_\infty} \right)^2 \mathbf{D}_{a2} \ddot{\mathbf{a}}, \quad (4b)$$

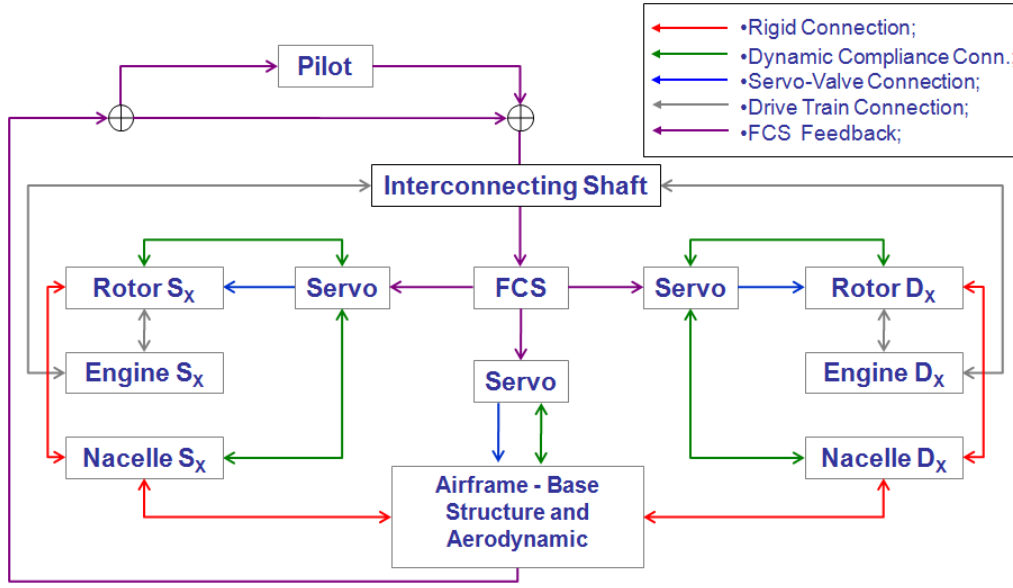


Figure 1: Block diagram of tiltrotor aeroservoelastic model.

where $\mathbf{a} = \{\mathbf{q}; \mathbf{v}_g\}$, by means of a rational approximation reduced to minimum states through a balanced truncation [11].

The resulting model coefficients can be modified to take into account known experimental data that may improve the quality of quasi-steady stability derivatives associated to rigid body modes and control surfaces.

Rotor Aeroelasticity

Linearized rotor modeling is more challenging than the airframe. In fact, in this case even the isolated structure cannot be considered linear, since it presents a significant dependence on the trim parameters \mathbf{p} [12]. The dependence on \mathbf{p} is magnified for unsteady aerodynamic forces. For this reason the aeroelastic models of the rotors have been considered as monolithic blocks composed by the joined structural and aerodynamic equations

$$\mathbf{A}_2(\mathbf{p})\dot{\mathbf{q}}_r + \mathbf{A}_1(\mathbf{p})\dot{\mathbf{q}}_r + \mathbf{A}_0(\mathbf{p})\mathbf{q}_r = \mathbf{B}_g(\mathbf{p})\mathbf{v}_g + \mathbf{f}_c(\mathbf{p}). \quad (5)$$

where \mathbf{q}_r are global rotor degrees of freedom chosen using the Ritz decomposition of Eq. (1) as discussed for the airframe, matrices \mathbf{A}_0 , \mathbf{A}_1 , \mathbf{A}_2 , \mathbf{B}_g are Linear Time Invariant (LTI), computed using coefficient averaging to eliminate any periodicity whenever the rotor is not in axial flow conditions [12], and vector \mathbf{f}_c represents the forces applied by the servo-actuators on the rotor to control the blade collective and cyclic pitch angles.

Eq. (5) represents a quasi-steady, LTI approximation of the rotor dynamics. The state \mathbf{q}_r contains an arbitrary number of rotor elastic modes, expressed in the non-rotating reference frame using the multi-blade transform [12], plus six rigid rotor motion modes used as *constraint modes* to connect the rotor to the corresponding airframe model with the CMS approach [9]. The linearized model can be generated using comprehensive rotorcraft solvers; CAMRAD/JA [3] has been used in this work.

The strong dependence of the matrices in Eq. (5) from the trim condition \mathbf{p} ideally requires to assemble a specific model for each flight condition considered during the aeroservoelastic analysis. This approach has not been considered suitable for the purpose of implementing a fast tool. On the contrary, a discrete database of linearized models has been defined for several trim conditions. A robust interpolation method is then used to estimate rotor models for any intermediate trim point. The rotor model can be re-computed at selected flight conditions, to verify the quality of the interpolation.

To achieve significant freedom in the choice of the reference conditions used to populate the database, a technique that allows interpolation starting from a set of point-wise scattered data has been selected. The Moving Least Square (MLS) approach meets this requirement.

Given a set of distinct data points \mathbf{x}_i in the space \mathbb{R}^d and an operator $\mathbf{L}(\mathbf{x})$ whose values are known at the data points, the techniques finds a polynomial approximation of order m $\mathbf{P}^*(\mathbf{x}) \in \Pi_m$ at point

\mathbf{x} by minimizing, among all $\mathbf{P} \in \Pi_m$, the flowing weighted least square error

$$\sum_i \|\mathbf{P}(\mathbf{x}) - \mathbf{L}(\mathbf{x}_i)\|_2^2 \phi(\|\mathbf{x} - \mathbf{x}_i\|_2), \quad (6)$$

where ϕ is a non-negative Radial Basis Function (RBF) [13]. Using compact support weight functions the problem can be confined, resulting in a very efficient technique that requires the solution of very small linear algebraic problems for each computational point \mathbf{x} . Exact interpolation can be achieved with $\phi(0) = \infty$. Additional details on the solution of the problem can be found in [13, 14].

Usually an initial model based on a compact database composed of few computed rotor model can be sufficient to frame the critical zones on the parameter space. Then, the inclusion of additional points in this zone can be used to gain additional precision for the simulation results.

Servo-actuators

Servo-actuators are modeled as equivalent transfer-functions. The transfer function of a servo-actuator usually describes the motion of a generic control surface, β , as a function of the requested motion, β_c , and of the generalized reaction force applied by the dynamics of the control surface itself, m_c , (see Refs. [15, 11]), namely

$$\beta = H_\beta(s) \beta_c + H_M(s) m_c. \quad (7)$$

In general, both the servo-valve and compliance dynamics are fully represented. The corresponding expression of the generalized force m_c applied to the controlled surface is

$$m_c = \frac{1}{H_M(s)} (\beta - H_\beta(s) \beta_c), \quad (8)$$

provided the dynamic compliance $H_M(s)$ is not strictly proper. Otherwise, a dynamic residualization up to second order can be applied without breaking the causality of the overall system, since the structural dynamics of the connected element is second order differential in time. The generalized force becomes

$$m_c = m_M s^2 \beta + c_M s \beta + \frac{1}{\hat{H}_M(s)} (\beta - H_\beta(s) \beta_c), \quad (9)$$

where $\hat{H}_M(s)$ is a proper transfer function. The resulting transfer functions need to be transformed in the time domain to obtain a state-space model of the actuator.

The actual motion of the control surface, β , is then expressed as a function of the structural

states, $\beta = \mathbf{U}_\beta \mathbf{q}$, and the transfer function is added to the problem using the Principle of Virtual Work (PVW), namely

$$\delta \mathcal{L}_M = \delta \beta^T m_c = \delta \mathbf{q}^T \mathbf{U}_\beta^T \frac{1}{H_M(s)} (\mathbf{U}_\beta \mathbf{q} - H_\beta(s) \beta_c). \quad (10)$$

Servo-actuators of airframe control surfaces like ailerons, flaps, elevators and rudders can be modeled with this approach. Rotor servo-actuators can be introduced as well by restoring the load path between the rotor pitch motion and the airframe structural dynamics. The formulation is presented for the collective pitch motion. With the multiblade transformation the generalized theory can be formulated for the complete rotor pitch motion, also considering the cyclic contributions.

The blade pitch dynamics equation is

$$\delta \mathcal{L}_M = \delta \vartheta^T I_f \ddot{\vartheta} + \delta \vartheta^T I_f \Omega^2 \vartheta + \delta(\vartheta - \vartheta_0)^T K_{T0}(\vartheta - \vartheta_0) + \delta x^T f_c, \quad (11)$$

where I_f represents the moment of inertia about the blade feathering axis, Ω is the rotor rpm, K_{T0} is the collective control chain stiffness, and f_c is the reaction force due to the servo-actuator; ϑ is the blade pitch angle, while ϑ_0 is the pitch angle commanded by the servo-actuator and x represents the servo actuator extension.

The contributions to the blade pitch equation are: (1) the feathering inertia $I_f \ddot{\vartheta}$, (2) the propeller moment $I_f \Omega^2 \vartheta$, (3) the restoring moment $K_{T0}(\vartheta - \vartheta_0)$, due to the flexibility of the control chain, and (4) the servo-actuator reaction force f_c .

The extension of the servo-actuator is a function of the structural states, $x = \mathbf{U}_x \mathbf{q}$, while the pitch angle ϑ_0 is related to the servo-actuator through the kinematic gear ratio η , so that $\vartheta_0 = \eta x = \eta \mathbf{U}_x \mathbf{q}$.

As in Eq. (8), the reaction force applied by the servo actuator is

$$f_c = \frac{1}{H_f(s)} (x - H_x(s) x_c), \quad (12)$$

considering the servo-valve dynamic $H_x(s)$ and the dynamic compliance $H_f(s)$. The displacement x_c requested to the servo-actuator is a function of the blade pitch request ϑ_c generated by the pilot/FCS by means of the inverse of the kinematic gear ratio, $x_c = \vartheta_c / \eta$. Equation (11) becomes

$$\begin{aligned} \delta \mathcal{L}_M = & \delta \vartheta^T I_f \ddot{\vartheta} + \delta \vartheta^T I_f \Omega^2 \vartheta \\ & + \delta(\vartheta - \eta \mathbf{U}_x \mathbf{q})^T K_{T0}(\vartheta - \eta \mathbf{U}_x \mathbf{q}) \\ & + \delta \mathbf{q}^T \mathbf{U}_x^T \frac{1}{H_f(s)} \left(\mathbf{U}_x \mathbf{q} - H_x(s) \frac{1}{\eta} \vartheta_c \right). \end{aligned} \quad (13)$$

The cross-coupling terms between the rotor pitch motion, the airframe structural dynamics and the servo-actuator dynamics are related to the control system load path, rebuilt along the different sub-components. Moreover, the pilot/FCS input allows to introduce the pilot/FCS feedback to perform closed loop aeroservoelastic analyses.

Generally, pitch/bending and pitch/gimbal kinematic couplings must be taken into account when restoring the control chain moment $m_{con} = K_{T0}(\vartheta - \vartheta_0)$. In this case

$$\vartheta_0 = \eta \mathbf{U}_x \mathbf{q} - \sum_i K_{p_i} q_{ei} - K_{p_G} \beta_G, \quad (14)$$

where the term $-K_{p_i} q_{ei}$ is the kinematic pitch/bending coupling due to control system and blade root geometry, and q_{ei} is the i^{th} bending degree of freedom of the rotor. Similarly, K_{p_G} is the pitch/flap coupling for the gimbal or teetering motion. Any effect of local nonlinearities of the actuator, like freeplay, saturation and deadband can be taken into account.

Additional components

Along with the basic aeroservoelastic elements, important additional components can be taken into account.

The rotor drive train can be modeled as a lumped parameters sub-component directly in the linearized model. Currently, the drive train model can only connect rotors with dynamic models of the engine. Future development will allow to close the feedback loop by connecting the drive train model with the airframe at the appropriate locations.

Sensors range from the direct extraction of the motion of a physical point as a function of the states of the system, to the inclusion of the dynamics of the sensor itself in the model. In the latter case, the transfer function of the sensor is added after transforming it in the time domain in state-space form. Although typically part of the FCS, notch filters represent a widely used tool that allows to avoid or fix spill-over problems caused by the coupling of the FCS with higher frequency structural dynamics modes. In fact, while the FCS is usually developed by avionics specialists according to inputs from flight mechanics specialists and test pilots, the possibility to quickly filter out undesired signals directly in the aeroelastic model, without requiring any intervention on the FCS model, represents an extremely useful feature. Notch filters are modeled by adding the related transfer function, transformed in state-space form, to the overall system model.

Pilots are known to represent a potential source of unintended introduction of excitations into aircraft by means of the primary controls, resulting in Pilot-Induced and Pilot Augmented Oscillations (respectively PIO and PAO)-like events [16]. Such components can be easily modeled as an additional blocks in MASST.

Flight Control System

The FCS represents the core of modern rotary-wing aircraft, significantly of tiltrotor. For the purpose of performing linear stability analysis, a linearized model of the FCS for specific flight conditions and operating modes is required. As an alternative, when performing time-marching analysis, an input-output relationship from generic non-linear models of the FCS, including the real hardware in a Hardware-In-the-Loop (HIL) simulation, can be used.

CURRENT RESULTS

This tool is currently used for the analysis of the ERICA tiltrotor configuration [17].

Component-wise cross-validations have been performed by comparing the results obtained using the presented tool with corresponding ones directly obtained from the software used to feed the tool. For example, results of direct modal analysis and flutter of the entire airframe obtained from NASTRAN are compared with results obtained by incorporating the airframe model in form of sub-components (the wing/fuselage, the nacelles, the control surfaces), using the state-space representation of the unsteady aerodynamics.

Models obtained by assembling sub-models (the airframe, each nacelle) obtained by CMS substructuring in a reference configuration have been analyzed in different configurations (different nacelle angles, different mass and mass distribution) and compared to direct FE eigenanalyses in the same contribution, resulting in either a fairly good agreement when comparing one-to-one cases (e.g. different nacelle angles), or in acceptably good approximations (e.g. different weight distributions).

Similarly, rotor stability results directly obtained from CAMRAD/JA using a pylon model consisting in NASTRAN's airframe modes are compared with results obtained with the tool, after switching off the airframe aerodynamics.

Further correlation has been obtained by comparing rotor performances and whirl flutter stability results with analogous results obtained us-

Table 1: Tiltrotor airframe properties

Aircraft Mode (426 rpm) - Locking Device Off	Short Name	Frequency	
Mode Name		Hz	/rev
Roll Fuselage - Antisymmetric Wing Chord	RF/AWC	2.1	0.3
Symmetric Wing Beam - Symmetric Tube Torsion	SWB/STT	2.7	0.3
Yaw Fuselage - Antisymmetric Beam Tail	YF/ABT	3.6	0.5
Symmetric Wing Chord	SWC	3.7	0.5
Symmetric Tube Torsion - Symmetric Wing Beam	STT/SWB	4.5	0.6
Antisymmetric Axial Tube - Tail Torsion	AAT/TT	5.1	0.7
Antisymmetric Axial Tube - Beam Tail	AAT/ABT	5.6	0.7
Antisymmetric Tube Torsion - Fin Torsion	ATT/FT	6.3	0.8
Symmetric Fuselage Bending	SFB	9.5	1.3
Symmetric Fuselage Bending - Symmetric Wing Torsion	SBF/SWT	12.1	1.7

ing the general-purpose multibody solver MBDyn
<http://www.mbdyn.org/>.

Tiltrotor Model Set-up

The entire work has been organized around two radically different approaches used for whirl flutter analysis: (1) linearized model analysis, performed using MASST; (2) nonlinear analysis using multibody models built in MBDyn, to verify the most significant results obtained with the linearized approach.

The stability analysis in MASST used:

- the integrated FE airframe model obtained from NASTRAN;
- the airframe unsteady aerodynamics obtained from NASTRAN using the DLM;
- rotor models obtained from CAMRAD/JA, for the linearized analysis approach;

The multibody model of the rotor, with the exact kinematics of the hub joints and a FE model of the hub and rotor blade flexibility based on nonlinear FE beams, coupled with a modal representation of the airframe structural model, has been generated in MBDyn.

The airframe FE model has been used to compute the structural modes of the whole aircraft. No symmetric/antisymmetric splitting has been considered, since the FE model is not perfectly symmetric.

Whirl flutter analyses have been performed considering different Gross Weight - CG configurations in aircraft mode, with the locking device in the on/off configurations.

Airframe Model. The airframe models are realized using the modal approach from NASTRAN

FE models. The set of modal displacements contains: (1) rigid body modes (fore/aft, lateral, plunge, roll, pitch, yaw); (2) control surface modes (flaps, ailerons, elevator and rudder); (3) normal modes, function of the bandwidth of interest (up to 15 Hz).

The whirl flutter instability can be reasonably analyzed considering modes up to 2/rev. Whirl flutter analyses have been performed with fixed control surfaces. However, control surface modes may be used in the future to study the aeroservoelastic behavior of the tiltrotor when servo-actuator dynamics is considered.

The main elastic modes that have been chosen for whirl flutter analysis are reported in Table 1, for the case with locking device off.

The unsteady aerodynamics of the airframe has been evaluated in the frequency domain using the NASTRAN DLM for the airframe base structure. The main wing and the empennages are represented using lifting surfaces, while the nacelles and the fuselage have been modeled as slender bodies.

The aerodynamic matrices have been evaluated for the values of reduced frequencies k and Mach numbers M_∞ to cover the flight envelope in aircraft mode.

Rotor Models. Rotor linear models in axial flow have been obtained using CAMRAD/JA models supplied by AgustaWestland. The ranges of trim conditions reported in Table 2 have been considered for linear rotor models. The active degrees of freedom, in multiblade coordinates, are:

- 3 bending modes, the first and the third in flap and the second in lead/lag (stiff in plane rotor);
- 2 torsion modes, the control chain and the blade elastic torsion ones;

Table 2: Rotor Trim

Mode	Ω rpm	ISA m	Power hp	Min V_∞ kts	Max V_∞ kts
A/C	426	0	0	100	370
A/C	426	0	0	100	370
A/C	426	8000	2400	100	370
A/C	426	8000	2400	100	370

- 2 gimbal modes, longitudinal and lateral;
- 6 pylon/hub rigid modes.

Each rotor in the database is characterized by 28 degrees of freedom, considering collective, gimbal, cyclic and reactionless modes.

Only the right counterclockwise rotor models are generated by CAMRAD/JA; left clockwise models are generated exploiting symmetry.

Coupling Approach for Rotor-Airframe Model

Linear State-Space Approach: MASST. A linear state-space aeroelastic model of the tiltrotor is built in MASST using the previously described ROMs.

The model is used to evaluate the aeroelastic stability in aircraft mode through classic flutter diagrams. All stability analyses are performed using a continuation procedure [18] that allows to follow the evolution of only the desired subset of eigen-solutions of the system for the different parameter values. In this case 5 symmetric and 5 skew-symmetric airframe modes are tracked using continuation.

Nonlinear Multibody Approach: MBDyn. In the non linear multibody model only the right counterclockwise rotor is modeled in MBDyn. Airframe pylon modes are introduced in the rotor model using a modal element. Considering only the right rotor, symmetric and antisymmetric cases are analyzed separately. To obtain the symmetric and the antisymmetric mode shapes:

- symmetric and antisymmetric modal displacements are obtained measuring the displacements of both right and left pylon nodes, extracting the symmetric and skew-symmetric

contributions as

$$\mathbf{U}_{sym}(x, z, \vartheta) = \frac{1}{2}(\mathbf{U}_l(x, z, \vartheta) + \mathbf{U}_r(x, z, \vartheta))$$

$$\mathbf{U}_{skw}(y, \phi, \psi) = \frac{1}{2}(\mathbf{U}_l(y, \phi, \psi) + \mathbf{U}_r(y, \phi, \psi))$$

$$\mathbf{U}_{sym}(y, \phi, \psi) = \frac{1}{2}(\mathbf{U}_l(y, \phi, \psi) - \mathbf{U}_r(y, \phi, \psi))$$

$$\mathbf{U}_{skw}(x, z, \vartheta) = \frac{1}{2}(\mathbf{U}_l(x, z, \vartheta) - \mathbf{U}_r(x, z, \vartheta))$$

where

- (x, z, ϑ) are the fore/aft, plunge and pitch motions of the pylons;
- (y, ϕ, ψ) are the lateral, roll and yaw motions of the pylons;
- the modal mass and the modal stiffness are divided by 2 to take into account the fact that only one half of the model is effectively represented in the overall model:

$$\frac{1}{2}\mathbf{U}_{sym}^T \mathbf{M} \mathbf{U}_{sym} \ddot{\mathbf{q}} + \frac{1}{2}\mathbf{U}_{sym}^T \mathbf{K} \mathbf{U}_{sym} \mathbf{q} = 0 \quad (16a)$$

$$\frac{1}{2}\mathbf{U}_{skw}^T \mathbf{M} \mathbf{U}_{skw} \ddot{\mathbf{q}} + \frac{1}{2}\mathbf{U}_{skw}^T \mathbf{K} \mathbf{U}_{skw} \mathbf{q} = 0 \quad (16b)$$

The division by 2 of the modal mass and of the modal stiffness presumes a perfectly symmetric model. In this case the model is not completely symmetric, so a small approximation is introduced. 5 symmetric and 5 antisymmetric airframe modes have been chosen for time response analysis. Rigid body modes are not considered. Figure 2 shows the rotor model realized in MBDyn, with the airframe modal element block.

The multibody model is only used for time marching simulations. The frequency and damping of the airframe modes can be estimated from time response analysis using standard methods. The one proposed in [19] has been used. Time responses have been obtained for:

- rotor hub forces: \mathbf{T} (thrust force), \mathbf{Y} (side force), \mathbf{H} (drag force);
- rotor hub moments: \mathbf{M}_x (roll moment), \mathbf{M}_y (pitch moment), \mathbf{Q} (torque);
- airframe modes: symmetric and antisymmetric modal participation factors.

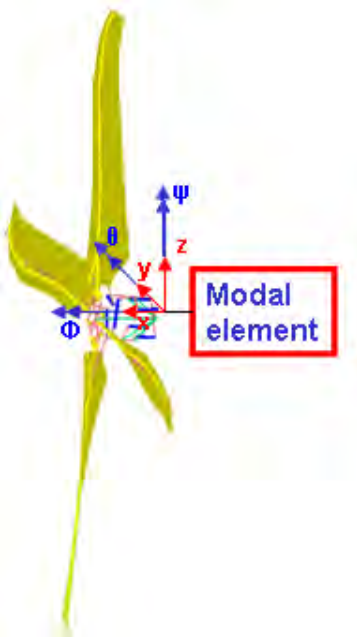


Figure 2: MBDyn rotor model.

WHIRL FLUTTER RESULTS

MASST has been used to compute the eigenvalues for the coupled airframe-rotor system in aircraft mode, as a function of airspeed at different: (1) gross weight - CG configurations, (2) locking device on/off state, (3) altitude, and (4) trim condition.

Critical conditions, without the effect of airframe unsteady aerodynamics, have been evaluated in MBDyn in order to verify the correct stability behavior of the tiltrotor.

The basic aircraft frequency and damping versus airspeed for the critical gross weight configuration, locking device off, at sea level standard conditions, with power off are shown in Figures 3–4. To verify the stability of the aircraft for the entire gross weight range, stability is also assessed at minimum weight. The symmetric tube torsion/symmetric wing bending (SWB/STT) mode is shown to be critical at 360 kts. Regulations require a 15% margin above the design speed for flutter clearance. The predicted point of instability is at a speed higher than that required for flutter clearance speed (320 knots). Consequently, the basic aircraft satisfies stability requirements.

The airframe unsteady aerodynamics effect has been evaluated and reported in Figures 5 using symmetric modes, and in Figures 6 using antisymmetric modes, compared with the previous analyses. The SWB/STT mode now becomes critical

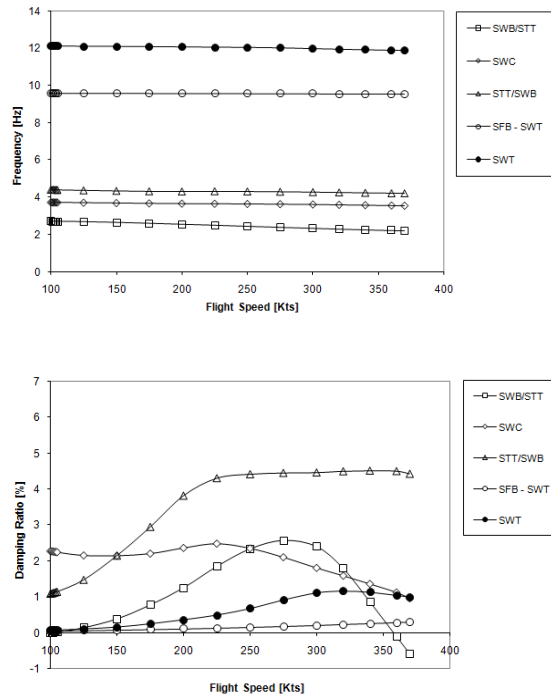


Figure 3: Eigenvalues vs airspeed of symmetric modes for max weight configuration, locking device off, power off at sea level.

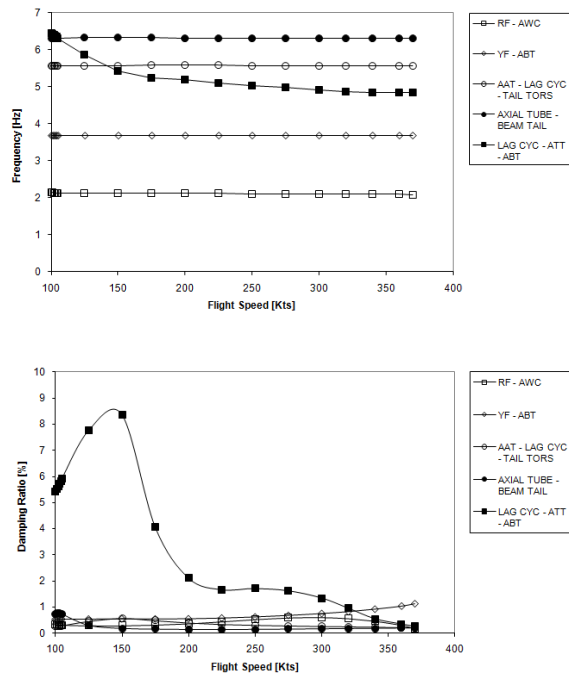


Figure 4: Eigenvalues vs airspeed of skew-symmetric modes for max weight configuration, locking device off, power off at sea level.

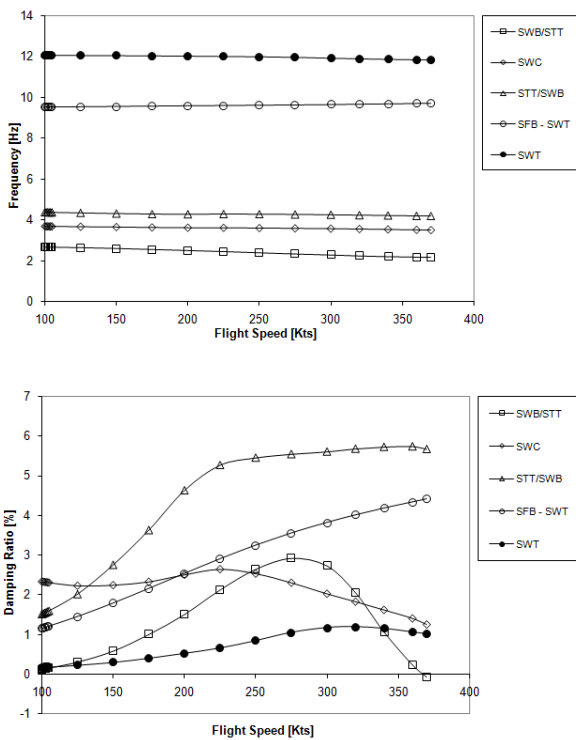


Figure 5: Eigenvalues vs airspeed of symmetric modes considering the effect of unsteady aerodynamics

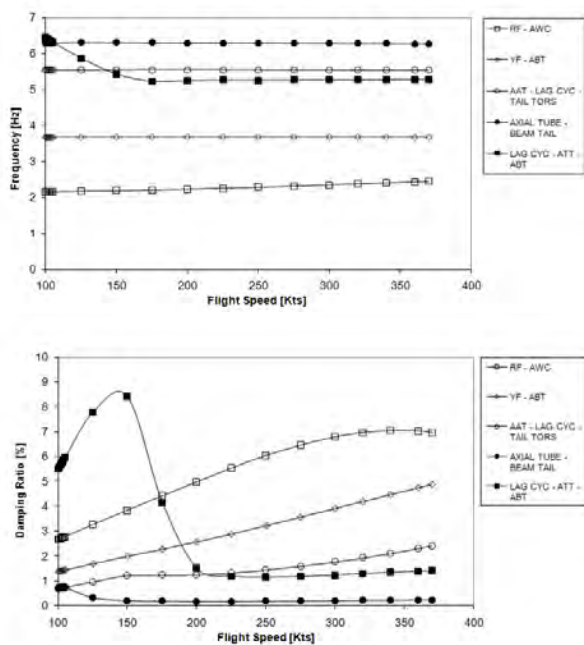


Figure 6: Eigenvalues vs airspeed of skew-symmetric modes considering the effect of unsteady aerodynamics

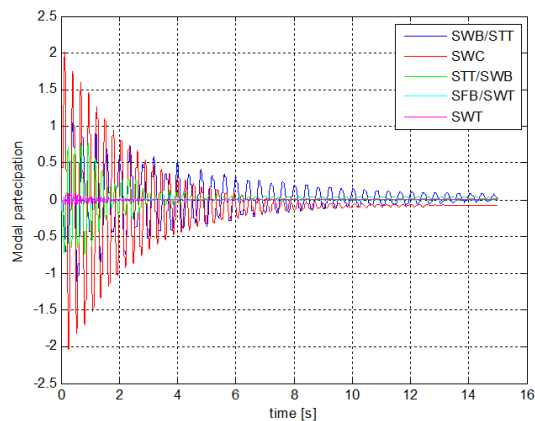


Figure 7: Time histories of modal participation coefficients during a multibody simulation at 200 kts, sea level, loking device off, zero power and maximum weight.

at 370 knots. The effect of airframe unsteady aerodynamics does not have a significant influence on the frequencies, but increases the damping of the symmetric and antisymmetric modes. In particular, the tail contribution significantly increases the damping of antisymmetric modes.

Multibody analyses confirm the linear analyses results obtained with the state-space model of the tiltrotor. The results are shown in Figures 7– 8.

FUTURE DEVELOPMENT

Future development will address the modeling of linear time-periodic subsystems. They are mainly intended to simulate rotors in non-axial flow, as occurs in the conversion corridor. The tool will be further validated by adding drive-train and pilot biomechanics models, and realistic servo and control system models. The capability to analyze rotor models in generic, non-axial flow conditions will allow to consider conventional helicopters in arbitrary reference flight conditions, to further assess its versatility.

ACKNOWLEDGMENTS

The authors acknowledge the support of AgustaWestland in extracting realistic rotor aeroelastic databases from CAMRAD/JA.

REFERENCES

[1] L. R. Stiles, J. Mayo, A. L. Freisner, K. H. Landis, and B. D. Kothmann. "Impossible to resist" the development

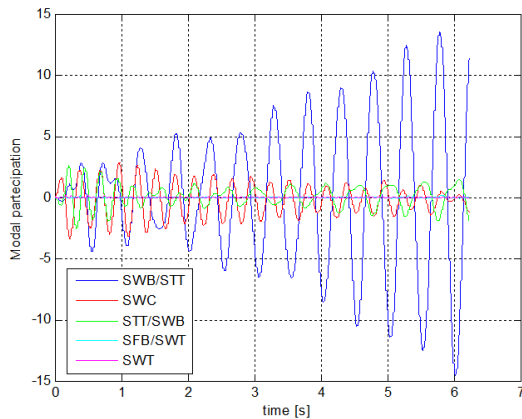


Figure 8: Time histories of modal participation coefficients during a multibody simulation at 360 kts, sea level, looking device off, zero power and maximum weight.

- of rotorcraft fly-by-wire technology. In *AHS 60th Annual Forum*, Baltimore, MD, June 8-10 2004.
- [2] M. Battipede, P.A. Gili, L. Carano, and V. Vaccaro. Constrained notch filter optimization for a fly-by-wire flight control system. *Aerotecnica Missili & Spazio*, 88(3):105–113, 2009.
 - [3] Wayne Johnson. Development of a comprehensive analysis for rotorcraft — I. rotor model and wake analysis. *Vertica*, 5:99–129, 1981.
 - [4] Wayne Johnson. Technology drivers in the development of CAMRAD II. In *American Helicopter Society Aeromechanics Specialists Conference*, San Francisco, California, January 19–21 1994.
 - [5] G. Bir and I. Chopra. University of Maryland Advanced Rotorcraft Code (UMARC) theory manual. UM-AERO 94–18, Center for Rotorcraft Education and Research, University of Maryland, College Park, MD, July 1994.
 - [6] B. Benoit, A.-M. Dequin, K. Kampa, W. von Grünhagen, P. M. Basset, and B. Gimonet. HOST, a general helicopter simulation tool for Germany and France. In *56th Annual Forum of the American Helicopter Society*, Virginia Beach, May 2000.
 - [7] P. Masarati, D.J. Piatak, G. Quaranta, J.D. Singleton, and J. Shen. Soft-inplane tiltrotor aeromechanics investigation using two comprehensive multibody solvers. *Journal of the American Helicopter Society*, 53:179–192, 2008.
 - [8] Tom Parham Jr. and Lawrence M. Corso. Aeroelastic and aeroservoelastic stability of the BA 609. In *25th ERF*, Rome, Italy, September 14–16 1999.
 - [9] Roy R. Craig, Jr. and Mervyn C. C. Bampton. Coupling of substructures for dynamic analysis. *AIAA Journal*, 6(7):1313–1319, July 1968.
 - [10] Luca Cavagna, Giuseppe Quaranta, and Paolo Mantegazza. Application of navierstokes simulations for aeroelastic stability assessment in transonic regime. *Computers & Structures*, 85(11–14):818–832, June-July 2007. doi:10.1016/j.compstruc.2007.01.005.
 - [11] M. Mataboni, G. Quaranta, and P. Mantegazza. Active flutter suppression for a three-surface transport aircraft by

recurrent neural networks. *Journal of Guidance, Control, and Dynamics*, 32(4), 2009.

- [12] Wayne Johnson. *Helicopter Theory*. Princeton University Press, Princeton, New Jersey, 1980.
- [13] D. Levin. The approximation power of moving least-squares. *Mathematics of Computation*, 67(224):1517–1531, 1998.
- [14] Giuseppe Quaranta, Pierangelo Masarati, and Paolo Mantegazza. A conservative mesh-free approach for fluid structure interface problems. In *Coupled Problems 2005*, Santorini, Greece, May 24–27 2005.
- [15] Herbert E. Merritt. *Hydraulic Control Systems*. John Wiley & Sons, New York, 1967.
- [16] Tom Parham Jr. and David Popelka. V–22 pilot-in-the-loop aeroelastic stability analysis. In *47th Annual Forum of the American Helicopter Society*, Phoenix, Arizona (USA), May 6–8 1991.
- [17] Fabio Nannoni, Giorgio Giancamilli, and Marco Cicalè. ERICA: the european advanced tiltrotor. In *27th ERF*, pages 55.1–15, Moscow, Russia, 11–14 September 2001.
- [18] Cesare Cardani and Paolo Mantegazza. Continuation and direct solution of the flutter equation. *Computers & Structures*, 8:185–192, 1976.
- [19] Giuseppe Quaranta, Pierangelo Masarati, and Paolo Mantegazza. Assessing the local stability of periodic motions for large multibody nonlinear systems using POD. *Journal of Sound and Vibration*, 271(3–5):1015–1038, 2004. doi:10.1016/j.jsv.2003.03.004.